Biophysical Chemistry 250 (2019) 106173

Contents lists available at ScienceDirect

Biophysical Chemistry

journal homepage: www.elsevier.com/locate/biophyschem

Mechanism of unfolding and relative stabilities of G-quadruplex and I-motif noncanonical DNA structures analyzed in biased molecular dynamics simulations

Tomasz Panczyk*, Patrycja Wojton, Pawel Wolski

Jerzy Haber Institute of Catalysis and Surface Chemistry, Polish Academy of Sciences, ul. Niezapominajek 8, 30239 Cracow, Poland

HIGHLIGHTS

- Telomeric i-motif and G-quadruplex are very stable at acidic pH.
- At neutral pH i-motif becomes weakened but does not unfold totally.
- Presence of G-quadruplex or its residues enhances the stability of i-motifs.
- G-quadruplex structure has weaker stabilizing effect than its unfolded residues.

GRAPHICAL ABSTRACT

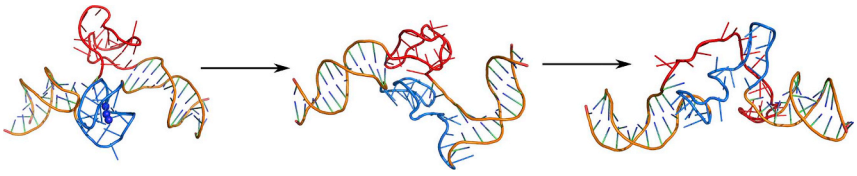

ARTICLE INFO

Keywords:
i-motif
G-quadruplex
Unfolding
Biased molecular dynamics

ABSTRACT

In this work we studied the unfolding processes of the noncanonical telomeric DNA fragments, i.e. G-quadruplex and i-motif. These transitions were analyzed in details by applying biased molecular dynamics simulations. The bias is imposed on the root of mean square displacement of selected atoms from the reference states which are ideal G-quadruplex and i-motif structures. The unfolding is carried out using the telomeric duplex fragment within which these both noncanonical structures are formed in the same place and exist together. The unfolding of one of the structures is carried out without affecting the second one. In the next stage of the studies the unfolding of the i-motif was also studied starting from the already unfolded G-quadruplex. We found that the work necessary to destroy G-quadruplexes are high at both acidic and neutral pH. The same was observed in the unfolding of i-motif at acidic pH. However, at the neutral pH the obtained work was small though still nonzero. It means that the presence of the complementary guanine rich strand enhances the stability of the i-motif which normally spontaneously unfolds to the hairpin at the neutral pH. Moreover, we found that unfolded G-quadruplex fragment is able to interact with the still existing i-motif and this leads to significant stabilization of the i-motif at the neutral pH. Thus, the presence of the complementary G-quadruplex at the neutral pH stabilizes the i-motif to some extent but even stronger stabilizing effect is observed after unfolding and relaxing the G-quadruplex.

1. Introduction

The noncanonical DNA structures that is, i-motif [1–9] and G-quadruplex [10–14] have recently been carefully studied using either experimental or computational techniques. [15–20] This is because the biological role of these structures appears to be more and more important as the research on them continues.

G-quadruplex may form in the guanine rich DNA strand. Moreover, when it forms in the 3′ overhang then it may itself be a DNA damage signal, producing responses analogous to those of other mediators of

* Corresponding author.
E-mail address: panczyk@vega.umcs.lublin.pl (T. Panczyk).

https://doi.org/10.1016/j.bpc.2019.106173
Received 21 March 2019; Received in revised form 12 April 2019; Accepted 12 April 2019
Available online 14 April 2019

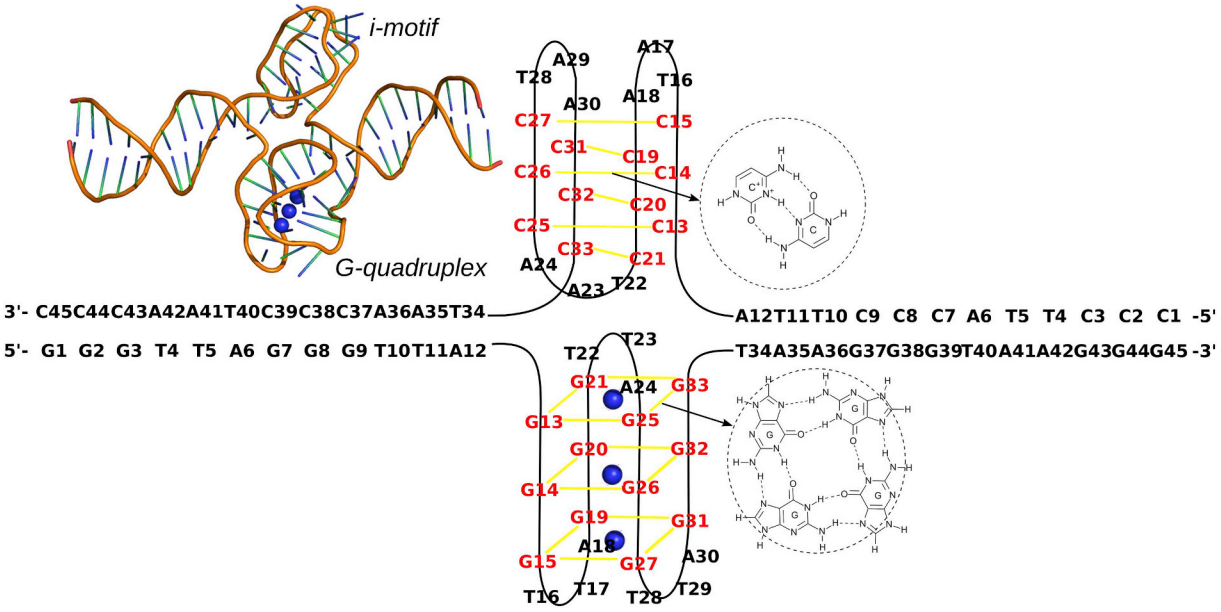

Fig. 1. Schematic representation (without preserving a particular folding symmetry) and visualization (inset on the l.h.s) of the iG structure analyzed in this study. The i-motif and G-quadruplex form due to corresponding bases pairing (Hoogsteen base pairing) shown in the insets on the r.h.s. G-quadruplex is additionally stabilized due to the presence of sodium ions (blue balls) localized in the centers of guanine quartets. (For interpretation of the references to color in this figure legend, the reader is referred to the web version of this article.)

telomere damage. [21,22] Additionally, the presence of G-quadruplex inhibits the telomerase activity [23] which is responsible for the reconstruction of the telomere length in cells reveling infinite proliferative capacity. Thus, the G-quadruplex stabilizing ligands are considered as selective inhibitors of cancer cell growth and it strongly suggests that induction of telomere shortening (or inhibition of telomerase activity) is a viable therapeutic strategy against cancer. [24,25]

More recently, increasing interest is being paid to the i-motif structure which can form in cytosine rich genome fragments, particularly in telomeres. [1,3] Biological role of i-motif is less recognized and it was believed that it can form only at reduced pH when the semiprotonated cytosine pairs can form. [3,4,26] However, very recently the evidence for i-motif formation in vivo has been provided by in cell NMR experiments [27] and the discovery of an antibody that binds i-motif specifically in the nuclei of human cells. [28] It was thus confirmed that i-motif can exist in regulatory regions of genome in living cells at physiological conditions. Recently, however, Chen et al. [4] described that carboxylated single-walled carbon nanotubes can selectively stabilize human telomeric i-motif DNA. Moreover, they found a subsequent inhibition of telomerase activity in the studied living cells. They proposed that the stabilization of the i-motif structure and the concomitant G-quadruplex formation lead to telomere uncapping and displacement of telomere-binding proteins, generating a DNA-damage response at telomeric level and subsequent cessation of tumor cell growth. [4]

G-quadruplex and i-motif are coupled in some way since they may form in the complementary regions of genome. However, in majority of cases these structure were studied independently and conclusions concerning their stabilization were rather limited to such factors like temperature, pH, presence of cations or molecular crowding conditions. There were also a few reports showing that these noncanonical DNA structures cannot exist together due to steric hindrance. [29,30] Though the mutual influence of both structures on their appearance and stabilization was understood [25] to our best knowledge these effects have not been adequately studied in the literature. In our recent paper we found that the presence of the G-quadruplex makes the i-motif containing cytosine-rich strand stable at the neutral pH though it was deteriorating spontaneously without the complementary guanine-rich and G-quadruplex containing strand. [31] We also found that iG structure (i-motif + complementary G-quadruplex structure) is relatively stable at neutral pH and the free energy barrier against i-motif unfolding/refolding is ca. 70 kJ mol^{-1}. This means that spontaneous unfolding of i-motif to the hairpin (and vice-versa) can occur at the neutral pH but the lifetime of each of these structures will be long enough to be observed experimentally [31].

The aim of this study is a more detailed analysis of the mutual influence of G-quadruplex and i-motif on their stabilities. To that purpose we will analyze the enforced unfolding processes and measure the work necessary to do such transitions in the presence or absence of the complementary structures and other conditions. As a collective variable, being a measure of the degree of the unfolding, we will use root of the mean squared displacement (rmsd) of the structures from the reference states which are the ideal i-motif or G-quadruplex structures. We believe that this choice of the collective variable minimizes the influence of added bias on the natural unfolding paths of the analyzed structures.

2. Methods

The analyzed iG structure (i-motif + G-quadruplex) has been composed by utilizing NAB (nucleic acid builder) language from AmberTools16 package [32] and using pdb files from the PDB database. The starting structure of the sequence [5′-GGG(TTAGGG)$_6$]: [5′-CCC(TAACCC)$_6$] has been build using NAB and next the atomic coordinates of the bases from 13 to 33 have been replaced by the corresponding coordinates from pdb files 2JPZ and 1EL2. The 1EL2 structure is a hybrid-type mixed parallel/antiparallel-stranded G-quadruplex (Hybrid-2) and this is intramolecular G-quadruplex structure of a biologically native, unmodified human telomeric sequence [33].

After initial optimization of the distances we obtained the structure iG shown schematically in Fig. 1. This is the telomeric fragment of chromosome with the noncanonical structures of i-motif and G-quadruplex placed symmetrically in the middle of the duplex. Obviously, we consider the situation when the i-motif and G-quadruplex are located in the same position on the duplex. This is the most intuitive arrangement since formation of either G-quadruplex or i-motif leaves the

complementary part of the duplex disordered. Then, it can naturally adopt an ordered complementary structure provided that all the necessary conditions are satisfied. In the case of the G-quadruplex it is the presence of Na+ or K+ ions, [34] for instance. I-motif, in turn, needs a reduced pH in order to produce protonated state of the cytosines. However, the reduction of pH cannot be strong since the full protonation of all cytosines leads again to an unstable state [1,6].

All calculations were based on the amber force field for nucleic acids [35] ff99 with the bsc1 modifications [36]. The constructions of the topologies were done using self-designed scripts and the force field was generated using the tleap program from the AmberTools16 package. We consider two cases of pH: neutral and acidic and this means that at the neutral pH all cytosines are in their standard unprotonated forms. The acidic pH means that we consider the cytosines 13, 14, 15, 19, 20 and 21 as additionally protonated. This was done by the tleap program with the included modification files for the creation of protonated cytosines. In the next step the systems were filled in TIP3P water molecules and suitable amounts of Na+ and Cl− ions were added in order to compensate the total charge and mimic physiological ionic strength of solution 0.145 mol L^{-1}. The number of water molecules was ca. 39,000, Na+ ions 196–202 (neutral – acidic), Cl− ions 114 and the total number of atoms in the simulation boxes was ca. 120,000. Three Na+ ions were used as cations stabilizing the G-quadruplex structure and were placed in the centers of guanine quartets. The choice of Na+ cation, instead of a more physiologically relevant K+, as central ion in the guanine quartets is justified since both cations are able to stabilize G-quadruplex at the considered temperature. [1]

The sizes of the simulation boxes were ca. 100 × 100 × 130 Å. The water molecules were kept rigid using the shake algorithm. [37] The calculations were carried out in NPT ensemble using 2 fs integration timestep and 12 Å cutoff distance for interatomic interactions was applied. The pressure and temperature were controlled using the Nose−Hoover barostat [38] with the relaxation times constants 2 ps and 0.2 ps for pressure and temperature, respectively.

All calculations were done using lammps molecular dynamics engine. [39] Every studied system was initially subjected to heating from 100 K to 310 K within 1 ns simulation time at a constant volume. Next, the equilibration runs were performed at constant temperature 310 K and pressure 1 atm for 2 ns. The final states from the equilibration runs were used as starting configurations in production runs. The production runs were based on the steered molecular dynamics since the considered systems reveal very slow motions in the unbiased calculations. We performed 50 ns of the unbiased calculations with the iG structure and found no visible unfoldings of either i-motif or G-quadruplex in both cases of i-motif protonation states.

Thus, in order to perform the enforced unfolding of either i-motif or the G-quadruplex we defined a collective variable which is the square root of the mean square displacement of atoms (rmsd) involved in formation of hydrogen bonds within the Hoogsteen pairs. These were all nitrogen and oxygen atoms connected by the dashed lines in Fig. 1. The displacement was measured from the reference (ref) state which is the iG structure taken from the last frame of the equilibration runs. It should be underlined that the rmsd was calculated after performing optimal rotation $U^{x_i(t)\rightarrow x_i^{ref}}$ that best superimposes the coordinates $x_i(t)$ onto a set of reference coordinates x_i^{ref}. That superimposition was done using the colvar [40] module linked to the lammps engine. The choice of the rmsd collective variable for enforcing the unfolding transitions is justified because it does not use a particular transition path and the system follows actually the easiest path which corresponds to a given rmsd value. The applied range of the moving rmsd restraint values was from 0 to 25 Å. Zero rmsd was the starting point corresponding to full overlapping of the coordinates with the reference state, while 25 Å was simply the value for which a total destruction of the analyzed structure has occurred. The rmsd restraint point was moving with the velocity 1.25 Å ns^{-1} and a single unfolding process corresponded to 20 ns of real time. The force constant responsible for dragging of the actual rmsd to its moving restraint point was 5 eV $Å^{-2}$ (115 kcal mol^{-1} $Å^{-2}$). The number of atoms to which the bias was applied was 48 in the case of G-quadruplex unfolding and 36 in the case of the i-motif unfolding.

It should be noted that the applied steered unfolding of the i-motif and G-quadruplex satisfies the conditions of Jarzynski inequality for computations of the free energy change. [41] However, in order to reproduce the free energy with an adequate quality a number of nonequilibrium unfolding transitions, started from the canonical distribution, should be performed and the free energy can then be determined as the exponential average. [42] However, this methods is useful when a single run takes not much time and many independent runs can be performed in a reasonable timescale. In our case a single unfolding transition takes a lot of time and therefore we cannot determine an exact free energy profile accompanied the unfolding transitions. Instead, we limit our considerations to comparative analysis of single runs which represent the work done during the enforced unfolding in nonequilibrium conditions. Thus, in that way we can compare the relative stabilities of the considered systems as functions of the parameters of choice.

Application of other enhanced sampling methods for determination of free energy profiles accompanying unfolding transitions was found as ineffective due to serious problems with the convergence. Either metadynamics or temperature accelerated metadynamics were unable to pass the rmsd collective variable in the reverse direction (refolding) which is necessary to reach the convergence. The applied approach based on Jarzynski inequality is physically consistent in this case and allows us to obtain reliable relative estimates of the work associated with the unfolding of those complex structures.

3. Results and discussion

The iG structure, as shown in the inset in Fig. 1, consists of 45 base pairs. In the middle of the initially existing Watson-Crick duplex the G-quadruplex and i-motif were formed in the guanine and cytosine rich strands, respectively. This structure is, as mentioned, either highly or significantly stable depending on the pH. [31] The unfolding of these noncanonical forms within the nanosecond timescale can thus be done only by applying biased simulations. Fig. 2 shows the snapshots of the iG structures after the enforced unfolding and relaxation of both the G-quadruplex and the i-motif at the neutral and acidic pH.

Analysis of Fig. 2 leads to a few qualitative conclusions, namely, it is easy to notice that the i-motif parts of the iG are well preserved after the destruction of the G-quadruplexes only at acidic pH. Definitely, the enforced unfolding of the G-quadruplex does not affect the structure of the i-motif when the third hydrogen bond exists within the C^+–C pairs. At the neutral pH the symmetry of the i-motif is rather loosely kept and we can state that stability of the i-motif without the complementary G-quadruplex is rather weak. The weakening of the i-motif structure can be due to the strain being associated with the enforced unfolding of the G-quadruplex but the main reason of such a behavior is the lack of the protonated cytosines and the third hydrogen bond at the neutral pH. [31]

On the other hand the G-quadruplex structure is preserved after destruction of the i-motif either at acidic or at the neutral pH. Moreover, the sodium ions, entrapped in the guanine quartets, stay for the whole simulation time at their places and no exchange of these ions with the bulk occurs. It is interesting to note that after the relaxation without biasing forces the i-motif parts tend to form hairpin structures. These structures are alternative to i-motif forms of the cytosine rich strand with similar stability, as found in our previous work. [31]

A more quantitative conclusions concerning the unfolding processes can be drawn from Fig. 3 which shows how the distances between atoms forming hydrogen bonds evolve in time. This figure shows only the cases of the G-quadruplexes unfolding at both pH conditions. However, no matter that the associated i-motif parts of the iG systems are not affected by the biasing potential, these parts of the iG are

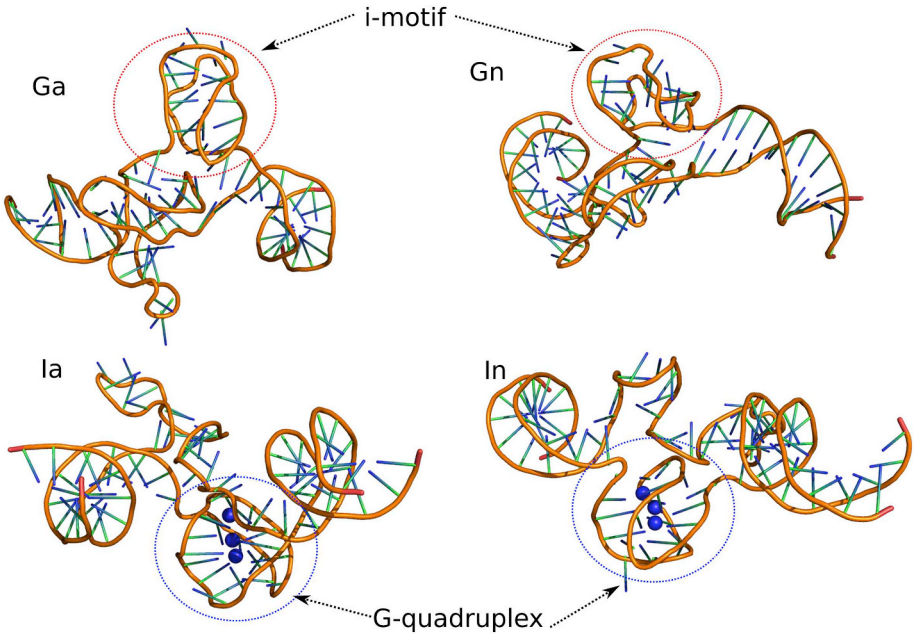

Fig. 2. Snaphosts of the iG structures after enforced unfolding during steered molecular dynamics followed by the relaxation without any bias for extra 20 ns. Ga: unfolding of the G-quadruplex at acidic pH; Gn: unfolding of the G-quadruplex at neutral pH; Ia: unfolding of the i-motif at acidic pH; In: unfolding of the i-motif at neutral pH.

affected by the processes of the G-quadruplexes unfolding. Obviously, the most visible changes of the distances occur within the G-quadruplexes as they are directly affected by the biasing potential. Another interesting observation concerns the sequence of the hydrogen bonds breaking. In the case of the neutral pH (parts (A) and (B)) the deterioration of the G-quadruplex starts from the innermost quartet (see Fig. 1) though 2 or 4 hydrogen bonds are still preserved until the end of the calculations.

It should be noted that the biasing force acts until 20th nanosecond of the calculation, the last 20 ns are without any bias and we can see a rapid drop of the distances and quite a fast stabilization around the new values. Of course a spontaneous refolding to G-quadruplex is highly unlikely within the available simulation time of the unbiased calculations. Thus, these new values can be treated as representative of transient but long lasting forms of the unfolded G-quadruplex. At acidic pH the unfolding of G-quadruplex proceeds in a different way though the pH cannot directly alter the G-quadruplex state. It can be seen that the unfolding starts from the opposite side, i.e. from the outermost guanine quartet. However, after 5 ns all quartets become partially broken though a few hydrogen bonds still exists until the end of the run. As seen in Fig. 2 in both cases of pH the sodium ions escaped from the cages formed by the G-qudruplexes and the final structures do not resemble G-quadruplexes at all.

Analysis of the i-motif structures during biased unfolding of G-quadruplexes leads to the conclusion that at acidic pH the i-motif is absolutely unaffected by that process. The hydrogen bonds within the i-motif are intact (Fig. 3D) and they only fluctuate around mean values. On the other hand, the i-motif at the neutral pH quickly lost its structure and most of hydrogen bonds become cleaved (particularly the outermost ones) as a result of the G-quadruplex unfolding. However, it seems that the obtained weakened i-motif structure is still stable as the distances only fluctuate around their mean values. On the other hand, the deterioration of the i-motif at the neutral pH was observed in the unbiased calculations but in the case of i-motif formed within the single stranded C-rich chain. [31] The presence of the complementary G-rich chain with the G-quadruplex formed needs crossing of ca. 70 kJ mol^{-1}

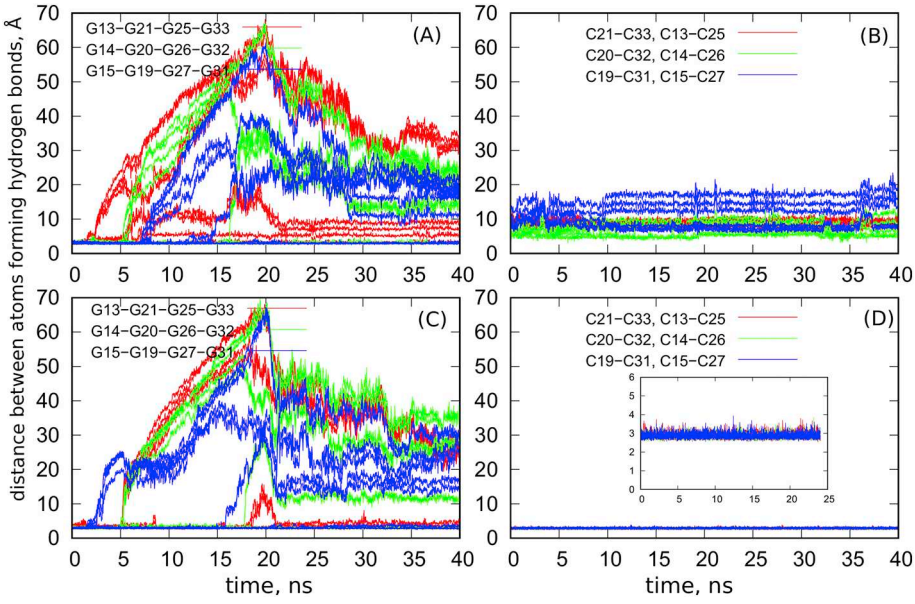

Fig. 3. Time evolution of the distances between atoms forming hydrogen bonds, as shown in Fig. 1, during enforced **unfolding of G-quadruplexes** at the neutral and acidic pH. Within each G-quartet there are 8 pairs of atoms forming hydrogen bonds and they are plotted using the same color. Similarly, the same color is used for the atoms pairs within the two neighboring doublets of bases in i-motifs, i.e. 6 lines. (A) distances between G-quadruplex forming atoms at the neutral pH, (B) distances between i-motif forming atoms at the neutral pH, (C) distances between G-quadruplex forming atoms at the acidic pH and (D) distances between i-motif forming atoms at acidic pH.

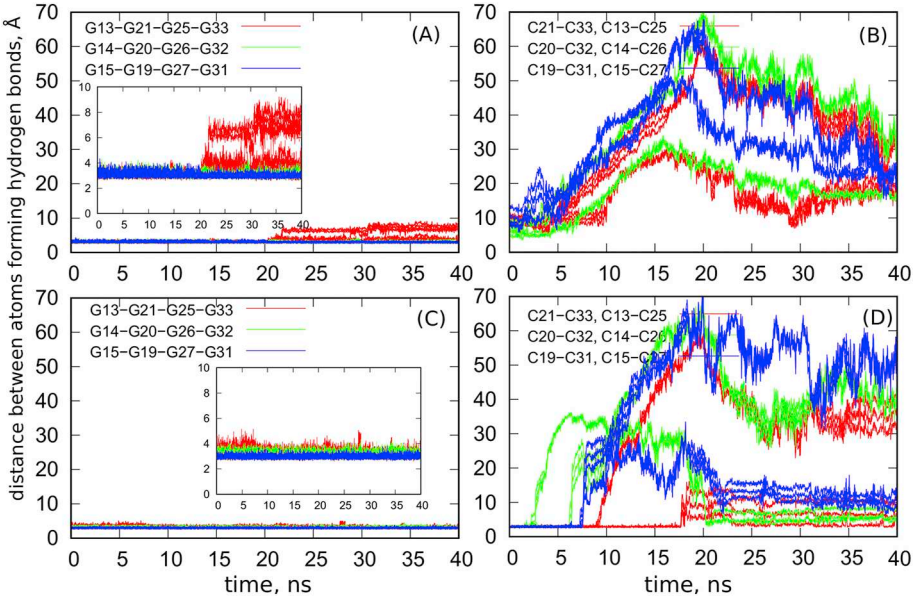

Fig. 4. Time evolution of the distances between atoms forming hydrogen bonds, as shown in Fig. 1, during enforced **unfolding of i-motifs** at the neutral and acidic pH. (A) distances between G-quadruplex forming atoms at the neutral pH, (B) distances between i-motif forming atoms at the neutral pH, (C) distances between G-quadruplex forming atoms at the acidic pH and (D) distances between i-motif forming atoms at acidic pH. Color codes are the same as in Fig. 3.

of free energy barrier in order to unfold the i-motif to hairpin. The enforced unfolding of G-quadruplex does not seem to significantly destabilize the complementary i-motif.

Fig. 4 shows how the distances between atoms forming hydrogen bonds change during enforced unfolding of i-motif parts of the iG structures. The organization of Fig. 4 is the same as Fig. 3 so we can directly observe the differences in the unfolding processes when the bias is added to the i-motif or to G-quadruplex parts of the iG systems. Thus, we can see that during enforced unfolding of the i-motifs the associated G-quadruplexes remain almost intact (note that the bias acts up to 20 ns). The i-motifs obviously undergo unfolding but it is clearly seen that pH affects the unfolding processes significantly. At the neutral pH all hydrogen bonds break at the very beginning (though some of them are already broken after the equilibration stage) and this means that the i-motif deteriorates as a whole structure. At the acidic pH the process proceeds in a different way. The deterioration of the i-motif begins from the middle pair of cytosines and next the outermost pairs undergo cleavage. The innermost pairs are the most resistant and they partially recover after removing of the biasing forces. In this case the i-motif seems to tend to hairpin form (see Fig. 2) contrary to the neutral pH case when the i-motif is spatially destroyed and all the distances from Fig. 4 are above 10 Å.

The enforced unfolding of the i-motifs do not affect the complementary G-quadruplexes, as seen in Fig. 4A and C. However, after removing the biasing force something unexpected happens to G-quadruplex at the neutral pH. Namely, the relaxation of the i-motif part seems to induce some deterioration of the G-quadruplex. Precisely, the hydrogen bonds between the innermost quartet of guanines break though the distances do not grow strongly. Moreover, visual inspection of the spatial structure of the G-quadruplex (Fig. 2, part In) does not show a significant deformation or deterioration of the G-quadruplex in this case. Thus, the observed increase of the distances in Fig. 4A occurred probably only incidentally and this is simply a transient state from which the hydrogen bonds spontaneously recover after some time.

Analysis of the work done during the enforced unfolding of both the i-motif and the G-quadruplex allows us to draw quantitative conclusions concerning the stabilities of these structures. Fig. 5 shows the work associated with the forces generated by the linearly increasing (with the constant velocity 1.25 Å ns^{-1}) rmsd in the case of the G-quadruplex unfolding.

As seen in Fig. 5 in both cases of pH the work necessary to destroy the G-quadruplexes are very similar. The curves reveal stepwise shape

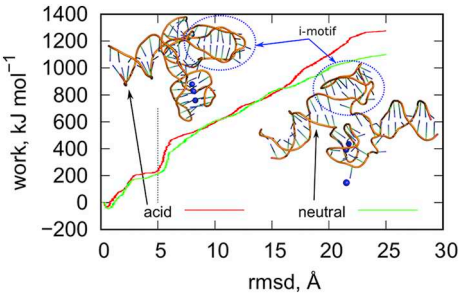

Fig. 5. The work measured during the enforced **unfolding of the G-quadruplexes** at the neutral and acidic pH. The biasing force (with the force constant 5 eV Å^{-2}) is imposed in the direction of the increasing root of mean squared displacement of atoms forming hydrogen bonds in each structure. The snapshots of the iG structures were taken after the first 4 ns of the unfolding and this point of time is indicated by the vertical dashed line.

with the most visible platteau within 3–5 Å of the rmsd (or 2.6–4 ns of the simulation time). The height of that first step is ca. 250 kJ mol^{-1} and this is associated with the cleavage of 3 hydrogen bonds, as seen in Fig. 3. However, in spite of the similarity between the plots in Fig. 5 the mechanism of the unfolding is different in these two cases. According to Fig. 3 the unfolding starts from the innermost guanine ring at the neutral pH and from the outermost in the case of the acidic pH. However, the energetic effect is very similar in both cases though it cannot be associated only with the hydrogen bonds cleavage. This is because the energies are much bigger than 3 times the energy of a single hydrogen bond, which is ca. 20 kJ mol^{-1}. [19]

The snapshots in Fig. 5 were taken at the end of the first platteau i.e. for 5 Å rmsd or 4 ns time. Thus, we can see that the state of the i-motif affects the mechanism of the G-quadruplex unfolding. At acidic pH the stiff structure of the i-motif does not affect the bottom part (the innermost) of the G-quadruplex and its deterioration begins from the outermost side. At the neutral pH, in turn, the i-motif seems to closely interact with the innermost part of the G-quadruplex and therefore its deterioration starts from that end. But the release of sodium cation occurred from the outermost guanine quartet though the hydrogen bonds in this part of the G-quadruplex were still present. This is quite unexpected observation and the release of Na^+ is probably due to some oscillations of the whole structure being the result of the breaking of the innermost guanine quartet.

The next step in the work plot in Fig. 5 around 5 Å corresponds to

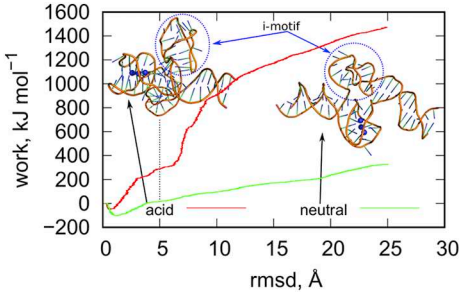

Fig. 6. The work measured during the enforced **unfolding of the i-motifs** at the neutral and acidic pH. The biasing force (with the force constant 5 eV Å^{-2}) is imposed in the direction of the increasing root of mean squared displacement of atoms forming hydrogen bonds in each structure. The snapshots of the iG structures were taken after the first 4 ns of the unfolding and this point of time is indicated by the vertical dashed line.

the cleavage of another groups of hydrogen bonds (6 at the neutral pH and 4 at the acidic pH). Further almost linear increase of the work is associated with the cleavage of other hydrogen bonds and, as seen in Fig. 3 they break faster in the case of the neutral pH. It seems that the G-quadruplex at the neutral pH is slightly less stable than at the acidic one though there are no direct reasons for the pH dependence of G-quadruplex.

Fig. 6 shows the work associated with the unfolding of i-motifs at the neutral and acidic pH. We can generally see large differences in the stabilities of the i-motifs depending on pH. At the acidic pH the work necessary to destroy the i-motif structure is very large and comparable to the unfolding of G-quadruplexes in Fig. 5. However, at the neutral pH the determined work is small; the total work associated with the full unfolding of the i-motif is not bigger than 420 kJ mol^{-1}. Thus, when we divide that value by the number of pairs potentially forming hydrogen bonds then the average work associated with the cleavage of a single hydrogen bond is ca. 23 kJ mol^{-1}. Of course, the determined work does not come from the hydrogen bonds only, also the stacking energies play a role so the average energy per single hydrogen bond is even smaller. Nevertheless, the unfolding of the i-motif needs some work to be delivered from the environment because otherwise the determined work in Fig. 6 would be negative. We can thus conclude that the stability of the i-motif at the neutral pH is significantly weakened but it does not unfold spontaneously. This observation is in agreement with our previous findings based on the metadynamics approach [31]. Simply, the presence of the complementary G-quadruplex stabilizes the i-motif to some extent.

The unfolding of the i-motif proceeds in similar fashion like the G-quadruplexes so we can notice a stepwise shape of the initial part of the work functions. These steps appear around 5 Å of the rmsd or 4 ns of the simulations time. Fig. 4 allows us to recognize that at the neutral pH this first step corresponds to the cleavage of all hydrogen bonds and next the deterioration proceeds further. However, at the acidic pH the step on the work plot corresponds to the cleavage of only 2 hydrogen bonds. Interestingly, these bonds are located in the middle part of the i-motif. Other bonds cleave sequentially but this is not clearly visible in the work plot because it grows monotonically without well resolved steps. The snapshots at 5 Å rmsd show that at these points the i-motif shapes are still well preserved.

The general conclusion coming from the above results is that at the acidic pH the iG structure is very stable and cannot unfold spontaneously. However, upon increasing pH up to physiological one, when the deprotonation of cytosines occurs, the stability of the iG will be weakened. Looking at Figs. 5 and 6 we can conclude that the most likely is the unfolding of i-motif while the G-quadruplex should stay intact. More precisely, full unfolding of the i-motif to the hairpin still needs some energy, as already mentioned. But weakening of the initial i-motif structure proceeds quickly and the weakened state (actually analyzed

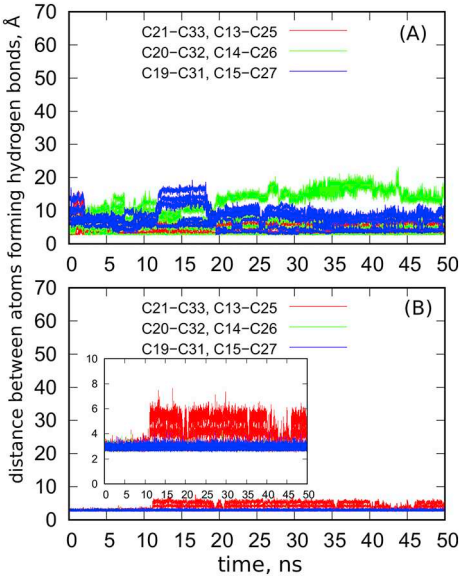

Fig. 7. Distances between atoms forming hydrogen bonds determined for i-motif structure in unbiased calculations. (A) neutral pH, (B) acidic pH. A single color is used for the representation of six various distances between atoms belonging to bases denoted in the legend.

here), though reveals substantial stability, will deteriorate before the G-quadruplex.

The stability of the i-motif at the neutral pH has been analyzed in our previous paper [31] by tracking the rmsd changes in unbiased calculations. Fig. 7 presents, just to confirm the conclusions drawn in [12], the changes in distances between atoms forming hydrogen bonds within the i-motif structures at both acidic and neutral pH. Fig. 7 shows actually analogous results like Figs. 3 and 4 but it concerns the iG structures without any bias added. So, the conclusions from Fig. 7 are obvious for the acidic pH. Namely, the i-motif is kept by many hydrogen bonds and it does not deteriorate within quite long simulation time reaching 50 ns. However, a few bonds break occasionally but they recover after some time. This happens for the bonds localized at the bottom of the i-motif.

At the neutral pH the i-motif is, as mentioned, weakened and this is confirmed by the distances shown in Fig. 7. Many hydrogen bonds disappeared as the distances are bigger than 3.5 Å, however there is still large number of distances around 3 Å which indicate the presence of hydrogen bonds. But the most important observation is that the distances fluctuate but do not grow above 20 Å. This means that the i-motif spatial shape is fairly well preserved at the neutral pH and it does not unfold totally. In ref. [31] we concluded that the i-motif at the neutral pH is stabilized by the presence of the G-quadruplex in the complementary guanine rich strand. However, the current study leads to some revision of the role of G-quadruplex in the stabilization of the i-motif.

Fig. 8A shows the results concerning the enforced unfolding of i-motifs but currently the starting and reference structures are the final states obtained after unfolding of the G-quadruplexes. These reference states are the Ga and Gn structures from Fig. 2 and the biases are added to i-motif parts in order to study unfolding of i-motifs when the G-quadruplexes do not exist any more. Similarly, Fig. 8B shows work measured during enforced unfolding of G-quadruplexes from the states where i-motifs have already been unfolded, i.e. states Ia and In from Fig. 2.

As seen in Fig. 8A the lack of G-quadruplex at acidic pH does not affect the stability of the i-motif. It is highly stable no matter whether there is the G-quadruplex formed in the complementary guanine rich strand or that part of the strand is in structural disorder. At the neutral pH, however, we observe quite surprising result. Namely, it seems that

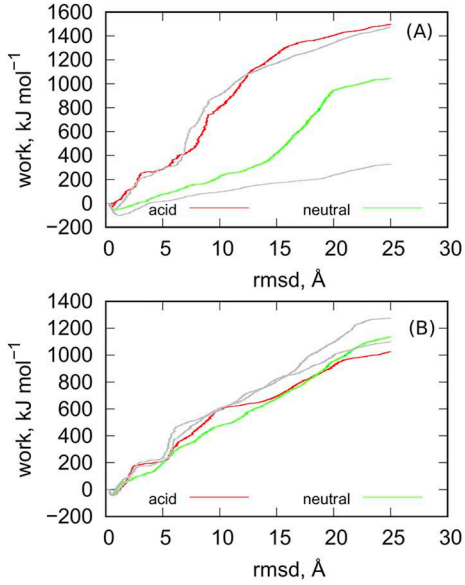

Fig. 8. Work measured during enforced unfolding of (A) i-motifs and (B) G-quadruplexes starting from the semi-unfolded iG structures shown in Fig. 2: (A) Ga and Gn, (B) Ia and In. The unfoldings were carried out in the same way like in Figs. 4 and 5 and the gray curves show, for comparison, results from these figures.

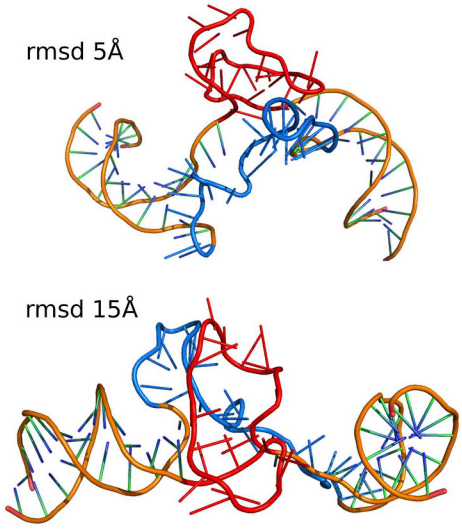

Fig. 9. The simulation snapshots taken at two rmsd values 5 and 15 Å during the enforced unfolding of i-motifs at neutral pH and initiated from the semi unfolded Gn structure from Fig. 2. The i-motif forming fragments are in red while the fragments which previously formed G-quadruplex are in blue. (For interpretation of the references to color in this figure legend, the reader is referred to the web version of this article.)

the structural disorder in the guanine rich strand stabilizes the i-motif when compared to the previous case of the presence of a perfect G-quadruplex structure. The work necessary to unfold the i-motif is significantly larger than that corresponding to the unfolding of i-motif from the ideal iG structure. Fig. 9 shows two simulation snapshots taken at rmsd 5 Å and 15 Å which help to understand why the presence of the unfolded G-quadruplex fragment stabilizes the i-motif stronger than the ideal G-quadruplex structure. As seen in Fig. 9 the i-motif is able to approach the spatially extended structure formed by the duplex fragment and the unfolded G-quadruplex. This enhances the pairwise interactions between the i-motif forming atoms and these belonging to the residues which formed G-qudruplex and duplex. Mutual interactions between atoms forming i-motif and G-quadruplex are stronger and stronger as the deterioration of the i-motif proceeds. Therefore, the work necessary to decompose the i-motif is higher and higher as the rmsd increases. In the original form of iG, as shown in the inset in Fig. 1, the i-motif is spatially well separated from the G-quadruplex and from the duplex, thus there are no extra interactions which enhance the stability of the i-motif.

The unfolding of the G-quadruplex from the semi unfolded state (Fig. 8B) needs very similar amount of work like the unfolding from the original iG structure (Fig. 5). Thus, the presence of i-motif little affects the stability of the complementary G-quadruplex. However, at the neutral pH the difference between work plots seen in Fig. 8B may suggest some small stabilizing effect of the i-motif. Nevertheless, any G-quadruplex unfolding process (acidic or neutral pH) starting from any initial structure is difficult and cannot occur spontaneously. The i-motif unfolding is definitely easier at the neutral pH and the presence of the unfolded and disordered G-quadruplex forming fragment significantly enhances the stability of the i-motif at the neutral pH.

4. Summary

The presented results of the analysis of the unfolding of G-quadruplex and i-motif, which may appear within the telomeric DNA region, led to several important conclusions. Namely, determination of the work necessary to unfold of these structures, in biased molecular dynamics involving steered rmsd increase, allowed us to state that G-quadruplexes are highly stable and their stability actually does not depend on the pH which indirectly comes through modification of the energetic state of the complementary i-motif. The unfolding of the G-quadruplex proceeds in quite different way depending on pH, namely at the neutral pH the deterioration starts from G13-G21-G25-G33 guanine quartet while at the acidic one G15-G19-G27-G31 quartet is destroyed first (see Fig. 1). The complementary i-motifs are unaffected by the enforced and strong structural changes in the G-quadruplexes.

The pH has strong influence on the stability of the i-motif, the determined work associated with the enforced unfolding of the i-motifs differ strongly. At the acidic pH the amount of work is comparable to the case of G-quadruplex unfolding but at the neutral pH the work is much smaller though still nonzero (or non negative). This means that the unfolding of i-motif at the neutral pH is relatively easy but still non spontaneous. Thus, the i-motif spatial structure, though significantly weakened, is preserved also at the neutral pH. This effect is assigned to the presence of the complementary G-quadruplex because, as found in our previous paper, the lack of the complementary guanine rich strand leads to spontaneous unfolding of the i-motif to hairpin structure. The stabilizing role of the G-quadruplex was investigated more closely and we concluded that the presence of the ideal G-quadruplex is less effective than its unfolded and disordered residues. This is because the G-quadruplex residues approach the i-motif more closely and enhance the interatomic interactions which, in turn, hinder the unfolding of the i-motif.

Acknowledgments

This work was supported by Polish National Science Centre grant 2017/27/B/ST4/00108.

The authors declare no competing financial interest.

References

[1] A.T. Phan, J.-L. Mergny, Human telomeric DNA: G-quadruplex, i-motif and Watson–Crick double helix, Nucleic Acids Res. 30 (2002) 4618–4625.
[2] H.A. Day, P. Pavlou, Z.A.E. Waller, i-Motif DNA: structure, stability and targeting with ligands, Bioorg. Med. Chem. 22 (2014) 4407–4418, https://doi.org/10.1016/j.bmc.2014.05.047.
[3] K. Gehring, J.-L. Leroy, M. Guéron, A tetrameric DNA structure with protonated cytosine-cytosine base pairs, Nature 363 (1993) 561–565, https://doi.org/10.1038/

363561a0.
[4] Y. Chen, K. Qu, C. Zhao, L. Wu, J. Ren, J. Wang, X. Qu, Insights into the biomedical effects of carboxylated single-wall carbon nanotubes on telomerase and telomeres, Nat. Commun. 3 (2012) 1074, , https://doi.org/10.1038/ncomms2091.
[5] M. Debnath, S. Ghosh, A. Chauhan, R. Paul, K. Bhattacharyya, J. Dash, Preferential targeting of i-motifs and G-quadruplexes by small molecules, Chem. Sci. 8 (2017) 7448–7456, https://doi.org/10.1039/C7SC02693E.
[6] B.G. Kim, T.V. Chalikian, Thermodynamic linkage analysis of pH-induced folding and unfolding transitions of i-motifs, Biophys. Chem. 216 (2016) 19–22, https://doi.org/10.1016/j.bpc.2016.06.001.
[7] J. Choi, S. Kim, T. Tachikawa, M. Fujitsuka, T. Majima, pH-induced intramolecular folding dynamics of i-motif DNA, J. Am. Chem. Soc. 133 (2011) 16146–16153, https://doi.org/10.1021/ja2061984.
[8] W. Ren, K. Zheng, C. Liao, J. Yang, J. Zhao, Charge evolution during the unfolding of a single DNA i-motif, Phys. Chem. Chem. Phys. 20 (2018) 916–924, https://doi.org/10.1039/C7CP06235D.
[9] Y. Peng, X. Wang, Y. Xiao, L. Feng, C. Zhao, J. Ren, X. Qu, i-Motif quadruplex DNA-based biosensor for distinguishing single- and multiwalled carbon nanotubes, J. Am. Chem. Soc. 131 (2009) 13813–13818, https://doi.org/10.1021/ja9051763.
[10] I. Russo Krauss, S. Ramaswamy, S. Neidle, S. Haider, G.N. Parkinson, Structural insights into the quadruplex–duplex 3′ interface formed from a telomeric repeat: a potential molecular target, J. Am. Chem. Soc. 138 (2016) 1226–1233, https://doi.org/10.1021/jacs.5b10492.
[11] D. Sen, W. Gilbert, Formation of parallel four-stranded complexes by guanine-rich motifs in DNA and its implications for meiosis, Nature 334 (1988) 364–366, https://doi.org/10.1038/334364a0.
[12] S. Balasubramanian, S. Neidle, G-quadruplex nucleic acids as therapeutic targets, Curr. Opin. Chem. Biol. 13 (2009) 345–353, https://doi.org/10.1016/j.cbpa.2009.04.637.
[13] A.E. Bergues-Pupo, I. Gutiérrez, J.R. Arias-Gonzalez, F. Falo, A. Fiasconaro, Mesoscopic model for DNA G-quadruplex unfolding, Sci. Rep. 7 (2017) 11756, , https://doi.org/10.1038/s41598-017-10849-2.
[14] S. Burge, G.N. Parkinson, P. Hazel, A.K. Todd, S. Neidle, Quadruplex DNA: sequence, topology and structure, Nucleic Acids Res. 34 (2006) 5402–5415, https://doi.org/10.1093/nar/gkl655.
[15] T. Panczyk, P. Wolski, Molecular dynamics analysis of stabilities of the telomeric Watson-Crick duplex and the associated i-motif as a function of pH and temperature, Biophys. Chem. 237 (2018) 22–30, https://doi.org/10.1016/j.bpc.2018.03.006.
[16] J. Smiatek, C. Chen, D. Liu, A. Heuer, Stable conformations of a single stranded deprotonated DNA i-motif, J. Phys. Chem. B 115 (2011) 13788–13795, https://doi.org/10.1021/jp208640a.
[17] J. Smiatek, A. Heuer, Deprotonation mechanism of a single-stranded DNA i-motif, RSC Adv. 4 (2014) 17110–17113, https://doi.org/10.1039/C4RA01420K.
[18] J. Smiatek, D. Janssen-Müller, R. Friedrich, A. Heuer, Systematic detection of hidden complexities in the unfolding mechanism of a cytosine-rich DNA strand, Phys. A Stat. Mech. Appl. 394 (2014) 136–144, https://doi.org/10.1016/j.physa.2013.09.030.
[19] A. Garabedian, D. Butcher, J.L. Lippens, J. Miksovska, P.P. Chapagain, D. Fabris, M.E. Ridgeway, M.A. Park, F. Fernandez-Lima, Structures of the kinetically trapped i-motif DNA intermediates, Phys. Chem. Chem. Phys. 18 (2016) 26691–26702, https://doi.org/10.1039/C6CP04418B.
[20] Y. Bian, W. Ren, F. Song, J. Yu, J. Wang, Exploration of the folding dynamics of human telomeric G-quadruplex with a hybrid atomistic structure-based model, J. Chem. Phys. 148 (2018) 204107, , https://doi.org/10.1063/1.5028498.
[21] F. d'Adda di Fagagna, P.M. Reaper, L. Clay-Farrace, H. Fiegler, P. Carr, T. von Zglinicki, G. Saretzki, N.P. Carter, S.P. Jackson, A DNA damage checkpoint response in telomere-initiated senescence, Nature 426 (2003) 194–198, https://doi.org/10.1038/nature02118.
[22] S. Neidle, Human telomeric G-quadruplex: the current status of telomeric G-quadruplexes as therapeutic targets in human cancer: G-quadruplexes as cancer drug targets, FEBS J. 277 (2010) 1118–1125, https://doi.org/10.1111/j.1742-4658.2009.07463.x.
[23] A.M. Zahler, J.R. Williamson, T.R. Cech, D.M. Prescott, Inhibition of telomerase by G-quartet DMA structures, Nature 350 (1991) 718–720, https://doi.org/10.1038/350718a0.
[24] A. De Cian, L. Lacroix, C. Douarre, N. Temime-Smaali, C. Trentesaux, J.-F. Riou, J.-L. Mergny, Targeting telomeres and telomerase, Biochimie 90 (2008) 131–155, https://doi.org/10.1016/j.biochi.2007.07.011.
[25] J. Amato, N. Iaccarino, A. Randazzo, E. Novellino, B. Pagano, Noncanonical DNA secondary structures as drug targets: the prospect of the i-Motif, ChemMedChem 9 (2014) 2026–2030, https://doi.org/10.1002/cmdc.201402153.
[26] A. Pagano, N. Iaccarino, M.A.S. Abdelhamid, D. Brancaccio, E.U. Garzarella, A. Di Porzio, E. Novellino, Z.A.E. Waller, B. Pagano, J. Amato, A. Randazzo, Common G-quadruplex binding agents found to interact with i-motif-forming DNA: unexpected multi-target-directed compounds, Front. Chem. 6 (2018) 281, https://doi.org/10.3389/fchem.2018.00281.
[27] S. Dzatko, M. Krafcikova, R. Hänsel-Hertsch, T. Fessl, R. Fiala, T. Loja, D. Krafcik, J.-L. Mergny, S. Foldynova-Trantirkova, L. Trantirek, Evaluation of the stability of DNA i-motifs in the nuclei of living mammalian cells, Angew. Chem. Int. Ed. 57 (2018) 2165–2169, https://doi.org/10.1002/anie.201712284.
[28] M. Zeraati, D.B. Langley, P. Schofield, A.L. Moye, R. Rouet, W.E. Hughes, T.M. Bryan, M.E. Dinger, D. Christ, I-motif DNA structures are formed in the nuclei of human cells, Nat. Chem. 10 (2018) 631–637, https://doi.org/10.1038/s41557-018-0046-3.
[29] Y. Cui, D. Kong, C. Ghimire, C. Xu, H. Mao, Mutually exclusive formation of G-quadruplex and i-motif is a general phenomenon governed by steric hindrance in duplex DNA, Biochemistry 55 (2016) 2291–2299, https://doi.org/10.1021/acs.biochem.6b00016.
[30] S. Dhakal, Z. Yu, R. Konik, Y. Cui, D. Koirala, H. Mao, G-Quadruplex and i-motif are mutually exclusive in ILPR double-stranded DNA, Biophys. J. 102 (2012) 2575–2584, https://doi.org/10.1016/j.bpj.2012.04.024.
[31] P. Wolski, K. Nieszporek, T. Panczyk, G-Quadruplex and I-motif structures within the telomeric DNA duplex. A molecular dynamics analysis of protonation states as factors affecting their stability, J. Phys. Chem. B 123 (2019) 468–479, https://doi.org/10.1021/acs.jpcb.8b11547.
[32] D.A. Case, T.E. Cheatham, T. Darden, H. Gohlke, R. Luo, K.M. Merz, A. Onufriev, C. Simmerling, B. Wang, R.J. Woods, The Amber biomolecular simulation programs, J. Comput. Chem. 26 (2005) 1668–1688, https://doi.org/10.1002/jcc.20290.
[33] J. Dai, M. Carver, C. Punchihewa, R.A. Jones, D. Yang, Structure of the Hybrid-2 type intramolecular human telomeric G-quadruplex in K+ solution: insights into structure polymorphism of the human telomeric sequence, Nucleic Acids Res. 35 (2007) 4927–4940, https://doi.org/10.1093/nar/gkm522.
[34] I. Turel, J. Kljun, Interactions of metal ions with DNA, its constituents and derivatives, which may be relevant for anticancer research, Curr. Top. Med. Chem. 11 (2011) 2661–2687.
[35] S.J. Weiner, P.A. Kollman, D.T. Nguyen, D.A. Case, An all atom force field for simulations of proteins and nucleic acids, J. Comput. Chem. 7 (1986) 230–252, https://doi.org/10.1002/jcc.540070216.
[36] I. Ivani, P.D. Dans, A. Noy, A. Pérez, I. Faustino, A. Hospital, J. Walther, P. Andrio, R. Goñi, A. Balaceanu, G. Portella, F. Battistini, J.L. Gelpí, C. González, M. Vendruscolo, C.A. Laughton, S.A. Harris, D.A. Case, M. Orozco, Parmbsc1: a refined force field for DNA simulations, Nat. Methods (2015), https://doi.org/10.1038/nmeth.3658.
[37] H.C. Andersen, Rattle: a "velocity" version of the shake algorithm for molecular dynamics calculations, J. Comput. Phys. 52 (1983) 24–34, https://doi.org/10.1016/0021-9991(83)90014-1.
[38] W. Shinoda, M. Shiga, M. Mikami, Rapid estimation of elastic constants by molecular dynamics simulation under constant stress, Phys. Rev. B 69 (2004), https://doi.org/10.1103/PhysRevB.69.134103.
[39] S. Plimpton, Fast parallel algorithms for short-range molecular dynamics, J. Comput. Phys. 117 (1995) 1–19, https://doi.org/10.1006/jcph.1995.1039.
[40] G. Fiorin, M.L. Klein, J. Hénin, Using collective variables to drive molecular dynamics simulations, Mol. Phys. 111 (2013) 3345–3362, https://doi.org/10.1080/00268976.2013.813594.
[41] C. Jarzynski, Nonequilibrium equality for free energy differences, Phys. Rev. Lett. 78 (1997) 2690–2693, https://doi.org/10.1103/PhysRevLett.78.2690.
[42] S. Park, K. Schulten, Calculating potentials of mean force from steered molecular dynamics simulations, J. Chem. Phys. 120 (2004) 5946, https://doi.org/10.1063/1.1651473.